Loss of myeloid cell-derived vascular endothelial growth factor accelerates fibrosis

Christian Stockmann[a,b], Yann Kerdiles[a], Marc Nomaksteinsky[a], Alexander Weidemann[a], Norihiko Takeda[a], Andrew Doedens[a], Antonio X. Torres-Collado[c], Luisa Iruela-Arispe[c], Victor Nizet[d], and Randall S. Johnson[a,1]

[a]Molecular Biology Section, Division of Biological Sciences, University of California, San Diego, CA 92093; [b]Institut für Physiologie, Universität Duisburg-Essen, D-45122 Essen, Germany; [c]Department of Molecular, Cell, and Developmental Biology, University of California, Los Angeles, CA 90095; and [d]Department of Pediatrics and Skaggs School of Pharmacy and Pharmaceutical Sciences, University of California, San Diego, La Jolla, CA 92093

Edited by Michael Karin, University of California, San Diego School of Medicine, La Jolla, CA, and approved January 15, 2010 (received for review November 16, 2009)

Tissue injury initiates a complex series of events that act to restore structure and physiological homeostasis. Infiltration of inflammatory cells and vascular remodeling are both keystones of this process. However, the role of inflammation and angiogenesis in general and, more specifically, the significance of inflammatory cell-derived VEGF in this context are unclear. To determine the role of inflammatory cell-derived VEGF in a clinically relevant and chronically inflamed injury, pulmonary fibrosis, we deleted the VEGF-A gene in myeloid cells. In a model of pulmonary fibrosis in mice, deletion of VEGF in myeloid cells resulted in significantly reduced formation of blood vessels; however, it causes aggravated fibrotic tissue damage. This was accompanied by a pronounced decrease in epithelial cell survival and a striking increase in myofibroblast invasion. The drastic increase in fibrosis following loss of myeloid VEGF in the damaged lungs was also marked by increased levels of hypoxia-inducible factor (HIF) expression and Wnt/β-catenin signaling. This demonstrates that the process of angiogenesis, driven by myeloid cell-derived VEGF, is essential for the prevention of fibrotic damage.

angiogenesis | fibrosis | hypoxia | inflammation

Pulmonary injury initiates a complex series of healing responses generally involving extensive inflammation (1). Among myeloid cells that infiltrate the lung during the inflammatory phase of pulmonary fibrosis, macrophages represent a major population that is also known for its ability to release large amounts of VEGF (2). The significance of angiogenesis, particularly expression of the angiogenic factor VEGF, in pulmonary fibrosis is a matter of controversy (3–5), however. In lung tissue, recent work has shown that delivery of VEGF can aggravate pulmonary fibrosis but alleviate pulmonary hypertension, highlighting the complexity of its role (6). However, it is not clear whether angiogenesis is a prerequisite for fibrogenesis or simply a bystander phenomenon without a causal relationship or if it is a necessary compensatory mechanism to prevent excessive fibrosis (3).

Hypoxia is believed to be a profibrotic stimulus that contributes to the development of fibrosis in multiple ways. Key mediators of cellular adaptation to hypoxia are hypoxia-inducible factors (HIFs), with HIF-1 and HIF-2 being the most extensively studied. HIF-1 and HIF-2 are basic helix-loop-helix transcription factors that consist of an oxygen-sensitive α-subunit and a constitutively expressed β-subunit (7). It has been shown in vitro that chronic hypoxia is a strong stimulus for collagen synthesis (8, 9), and many genes involved in the remodeling of extracellular matrix and epithelial-to-mesenchymal transition are known HIF target genes (10); in turn, HIFs have been suggested to be involved in the development of tissue fibrosis (11). Besides the regulation of genes involved in angiogenesis, oxygen transport, and glucose metabolism (12), hypoxia and HIFs have been shown to affect Wnt/β-catenin signaling (13, 14), and the canonical Wnt/β-catenin pathway regulates crucial processes like fibroblast proliferation, myofibroblast differentiation, and epithelial-to-mesenchymal transformation, and is therefore a major pathway in the development of tissue fibrosis (5, 15–18).

A key question is thus the extent to which angiogenesis, driven by inflammation in pulmonary injury, is beneficial or detrimental to this process, whether it acts to alleviate tissue hypoxia following damage and injury, and whether it contributes to the fibrosis that results from chronic inflammation of damaged tissues. To address these questions, we used a tissue-specific deletion of the angiogenic factor VEGF-A in myeloid lineage cells to determine how expression of VEGF-A by cells of the innate immune system affects the process of fibrosis. We found that VEGF-A expression by myeloid cells is a crucial aspect of endothelial restoration and reepithelialization and that fibrosis is significantly accelerated in its absence.

Results

Loss of VEGF-A in Myeloid Cells Increases Pulmonary Fibrosis in Bleomycin-Treated Animals. To define the role of VEGF in the inflammatory response to pulmonary injury and fibrosis better, we created a targeted deletion of VEGF in cells of the myeloid lineage. Mice with both alleles of exon 3 of VEGF-A flanked by loxP sites ($VEGF^{+f/+f}$) (19) were crossed into a background of Cre recombinase expression driven by the lysozyme M promoter (LysMCre/$VEGF^{+f/+f}$) (20). This results in a tissue-specific deletion of the VEGF gene in mutant (Mut) mice, with excision in greater than 80% of isolated neutrophils or peritoneal macrophages (21, 22).

In the lung, aberrant healing responses to injury are thought to contribute to the pathogenesis of pulmonary fibrosis (1). We assessed the impact of myeloid cell-derived VEGF on vascular remodeling and tissue repair in an established lung injury model that provokes profound pulmonary fibrosis. On i.p. administration of bleomycin, VEGF Mut mice showed aggravated histological signs of pulmonary fibrosis and a marked increase in collagen deposition compared with WT littermates (Fig. 1 *A* and *B*). To determine whether the aggravated histopathological signs of pulmonary fibrosis seen in VEGF Mut animals translate into a physiologically relevant phenotype that affects the pulmonary gas exchange, we measured the oxygen uptake at the anaerobic threshold of WT and VEGF Mut animals treated with saline or bleomycin. Consistent with our histological findings, the oxygen uptake in VEGF Mut mice treated with bleomycin was significantly reduced (Fig. 1*C*), further indicating that the advanced fibrotic changes in these animals represent a major diffusion

Author contributions: C.S. and R.S.J. designed research; C.S., Y.K., M.N., A.W., N.T., A.D., A.X.T.-C., L.I.-A., V.N., and R.S.J. performed research; C.S., L.I.-A., V.N., and R.S.J. analyzed data; and C.S. and R.S.J. wrote the paper.

The authors declare no conflict of interest.

This article is a PNAS Direct Submission.

[1]To whom correspondence should be addressed. E-mail: rsjohnson@ucsd.edu.

This article contains supporting information online at www.pnas.org/cgi/content/full/0912766107/DCSupplemental.

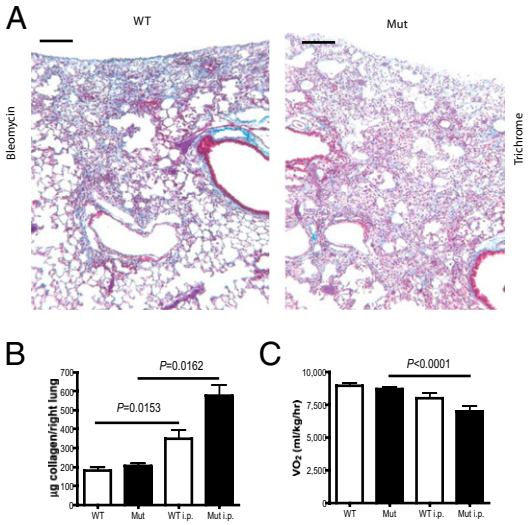

Fig. 1. Deletion of VEGF in myeloid cells leads to increased fibrosis and collagen deposition after pulmonary injury. (*A*) Trichrome staining of lungs from mice treated i.p. with bleomycin (10 mg/kg twice a week) after 28 days. VEGF Mut mice lacking VEGF in myeloid cells show aggravated histopathological signs of fibrosis. (*B*) Collagen assay from the entire right lung of Mut mice and littermate WT mice 28 days after i.p. bleomycin injection or treatment with saline (n = 5–7). (*C*) Assessment of oxygen uptake (VO_2) at the anaerobic threshold of Mut and WT mice 21 days after i.p. bleomycin injection or treatment with saline (n = 5). Error bars show SEM. (Scale bars: 100 μm.)

barrier that hampers the gas exchange within the alveolary-capillary unit.

Increase in Myofibroblast Formation in Mut Lung Tissue. A histopathological hallmark of pulmonary fibrosis is a massive increase of fibroblasts and myofibroblasts in the injured lung tissue, with concurrent loss of type II pneumocytes (1). We performed immunofluorescence for the fibroblast marker fibroblast-specific protein-1 (FSP) (Fig. 2*A*), the myofibroblast marker α-smooth muscle actin (SMA), and the type II pneumocyte marker thyroid transcription factor 1 (TTF-1) (Fig. 2*C*) on lung sections from saline-treated and bleomycin-treated (administered i.p.) animals. Quantitative analysis of each marker revealed higher numbers of fibroblasts as well as myofibroblasts and a significant loss of type II pneumocytes in VEGF Mut animals relative to WT littermates (Fig. 2 *B* and *D*). These observations corroborate the earlier histopathology and collagen deposition results, indicating that a much more rapid and extensive progression of pulmonary fibrosis occurs in animals lacking VEGF in their myeloid cells.

Loss of VEGF-A in Myeloid Cells Does Not Affect Infiltration. To determine whether the deletion of VEGF in myeloid cells affects their ability to infiltrate pulmonary tissue after injury, we analyzed myeloid cell populations in bleomycin-treated WT and VEGF Mut animals by immunohistochemistry as well as by flow cytometry of single-cell suspensions from fibrotic lungs. Although an increase of various cells from the myeloid lineage (particularly macrophages) was observed in each case, the levels and distribution of cell recruitment were similar in the WT and VEGF Mut animals (Fig. S1). Thus, the ability of macrophages to migrate into pulmonary tissues is not significantly influenced by their ability to release VEGF.

VEGF-A Levels and Endothelial Numbers Are Significantly Reduced in Mutants Postinjury. Pulmonary fibrotic lesions frequently exhibit a heterogeneous increase in vessel density, and an extant and important question is whether the release of angiogenic factors enables the development of fibrosis or, conversely, if it is a compensatory mechanism to prevent more severe fibrotic changes (3, 5, 6). Detection of VEGF protein by Western Blot analysis in whole-lung lysates revealed markedly elevated VEGF levels after intraperitoneal bleomycin treatment (i.p.) of WT mice compared with either untreated mice or bleomycin-treated VEGF Mut mice (Fig. 3 *A* and C). This latter observation demonstrates that an essential source of VEGF in the injured tissues derives from the infiltrating myeloid cells. This finding is in striking contrast to quantification of VEGF origin in solid tumors, where we have shown that VEGF from myeloid cells is an insignificant contributor to total tissue VEGF levels (22). Along with elevated VEGF levels, we detected an increase in phosphorylation of VEGF receptor 2 (VEGFR2) in fibrotic lung tissue, as assessed by detection of phosphotyrosine residues after immunoprecipitation of VEGFR2; this assay can be used as a measurement of receptor activation, and loss of VEGF in myeloid cells resulted in reduced activation of VEGFR2 in lungs (Fig. 3 *B* and *D*).

To determine whether the genotype-specific differences in VEGF levels and VEGFR2 activation translate into alterations of vascularization, we performed an analysis of vascular density on treated and untreated lungs. As shown in Fig. 3 *E* and *F*, treatment of WT mice with bleomycin (i.p.) results in a typical pattern of heterogeneous increases in blood vessel density along the periphery of fibrotic lesions and vascular rarefaction in the center of fibrotic foci. However, in VEGF Mut mice treated with bleomycin (i.p.), this increase in vascular density was significantly reduced (Fig. 3 *E* and *F*).

We hypothesized that the formation of previously undetected blood vessels seen in WT animals is a compensatory mechanism to enable tissue repair, restore tissue homeostasis, and prevent fibrosis. Interestingly, many processes leading to tissue fibrosis can be induced or triggered by hypoxia. For instance, it has been shown that pulmonary fibroblasts proliferate in response to low oxygen concentrations (23). Hypoxia, acting in large part through the HIFs, is also involved in the process of epithelial-to-mesenchymal transition and myofibroblast differentiation (24). Thus, impaired angiogenesis in Mut animals could result in inadequate tissue perfusion and oxygen delivery within fibrotic foci, thereby accelerating the progression of pulmonary fibrosis.

Expression of HIFs and Hypoxia Markers Is Elevated in Lungs from VEGF-Mut Animals Postinjury. An analysis of nuclear extracts from whole lungs showed that in saline-treated animals, HIF-1α as well as HIF-2α remained almost undetectable. In bleomycin-treated (i.p.) mice, lungs from WT animals showed a marked induction of HIF-1α as well as HIF-2α; however, the nuclear amount of both HIF isoforms was increased even further in lungs from VEGF Mut animals (Fig. 4 *A*–*C*). Furthermore, simultaneous immunodetection of $CD34^+$ vasculature and the HIF-regulated enzyme and hypoxia marker carbonic anhydrase IX (CA-IX) revealed CA-IX expression in fibrotic regions, which was, again, more pronounced in lungs from VEGF Mut animals compared with WT controls (Fig. 4*D*). It is noteworthy that within fibrotic lesions, the hypoxia and HIF-regulated gene CA-IX was particularly enhanced in its expression in areas that showed capillary rarefaction (Fig. 4*D*).

Increased Activation of Wnt/β-Catenin Signaling in Fibrotic Lungs from Mut Animals. Among various signaling pathways that are involved in the development of pulmonary fibrosis, the Wnt/β-catenin pathway has been determined to be of major importance; it is linked to crucial fibrotic processes, including proliferation of pulmonary fibroblasts and their differentiation into myofibroblasts (5, 16–18). It has also been reported that Wnt/β-catenin signaling can be triggered by hypoxia in an HIF-dependent manner (13, 14). As shown in Fig. 4*E*, nuclear extracts from bleomycin-treated (i.p.) lungs of WT mice show an

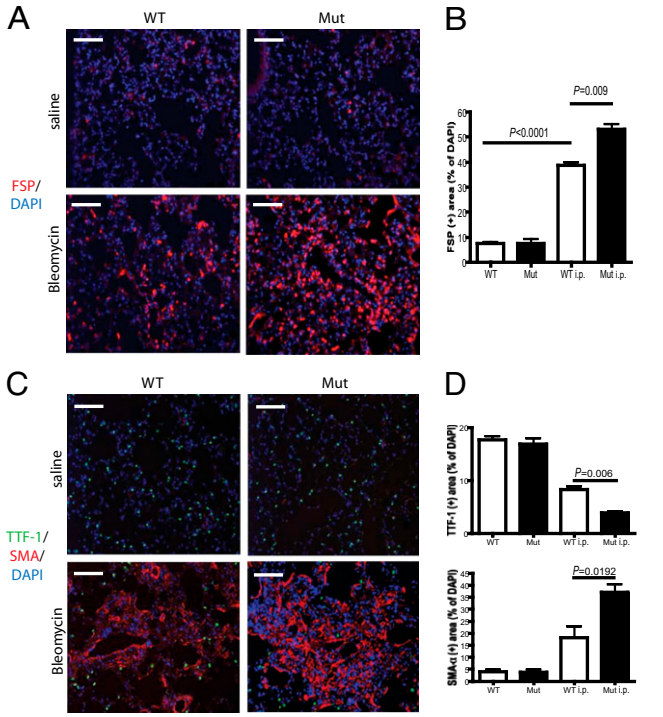

Fig. 2. Loss of myeloid cell-derived VEGF results in higher numbers of fibroblasts and myofibroblasts as well as a decrease in type II pneumocytes after pulmonary injury. (*A*) Detection of fibroblasts positive for the marker FSP in lungs from Mut and WT mice 28 days after i.p. bleomycin injection or treatment with saline. (*B*) Quantitative analysis of the area in pixels covered by FSP within lung sections from Mut and WT mice 28 days after i.p. bleomycin injection or treatment with saline (n = 4). (*C*) Simultaneous immunodetection of myofibroblasts and type II pneumocytes with the specific markers SMA and TTF-1 in lungs from Mut and WT mice 28 days after i.p. bleomycin injection or treatment with saline. (*D*) Quantitative analysis of the area in pixels covered by SMA and TTF-1 within lung sections from Mut and WT mice 28 days after i.p. bleomycin injection or treatment with saline (n = 4). Error bars show SEM. (Scale bars: 100 μm.)

increase in β-catenin protein levels compared with saline treatment, indicating increased translocation of β-catenin from the cytoplasm to the nucleus, a crucial step during β-catenin signaling (25, 26). A quantitative analysis demonstrates that nuclear levels of β-catenin are greatly increased in lungs from bleomycin-treated (i.p.) VEGF Mut mice relative to WT mice (Fig. 4*F*).

Similar results were seen in the expression of cyclin D1, a major downstream component of the Wnt/β-catenin signaling pathway (27). Whereas cyclin D1 was almost undetectable in nuclear extracts from saline-treated animals, bleomycin-treated (i.p.) WT animals showed increased cyclin D1 protein levels in their lungs, and the amount of cyclin D1 was elevated significantly further in lungs from VEGF Mut mice (Fig. 4 *E* and *G*). Consistent with enhanced Wnt/β-catenin signaling, we observed decreased levels of the epithelial marker E-cadherin in the cytoplasmic fraction in lungs from VEGF Mut animals (Fig. 4 *E* and *H*).

Discussion

In this work, we show that the specific deletion of VEGF in myeloid cells results in aggravated fibrosis and increased collagen deposition, indicating that inflammatory cell-derived VEGF is required for vascular remodeling after pulmonary injury and that this remodeling process acts to restore tissue homeostasis to prevent the development of pulmonary fibrosis.

Furthermore, we report that mutants had greatly decreased overall levels of VEGF within injured tissues, with diminished activation of VEGFR2 and impaired angiogenesis. This argues that myeloid cells are an indispensable source of VEGF after pulmonary injury and during pulmonary fibrosis. Interestingly, macrophages and type II pneumocytes represent the two major sources of VEGF in the lung. However, we observed a progressive loss of type II pneumocytes after bleomycin-induced injury. This is tantamount to the loss of one major source of VEGF in the lung, leaving myeloid cells, particularly macrophages, as the remaining potent source of VEGF. Consistently, after deletion of VEGF in myeloid cells, we observed a dramatic drop in overall VEGF levels.

In contrast, previous studies using various approaches, including small molecule inhibitors, to inhibit angiogenesis in general and VEGF signaling in particular reported reduced pulmonary fibrosis (28–30). It is important to mention that the time point of VEGF inhibition in these studies is restricted to the early event of initial pulmonary injury or VEGF inhibition is more broadly enacted beyond the inhibition of angiogenesis. Furthermore, some of the compounds used in these studies do not exclusively inhibit VEGF signaling but have effects on PDGF receptor and basic FGF signaling (28).

One point to consider in reconciling these results is that in the study by Chaudhary et al. (28), inhibitor compounds were administered simultaneously with bleomycin. During pulmonary injury, vascular leakage and the onset of the coagulation cascade are likely key initiating events leading to inflammation and subsequent fibrosis. Thus, it is possible that VEGF inhibitors in those experiments act to inhibit early damage and prevent or slow pulmonary fibrosis in this way; in this case, such treatment would outweigh or mask effects of VEGF inhibition on the subsequent repair process. In our models, the deletion of VEGF is restricted to infiltrating myeloid cells, and thus becomes effective after initial pulmonary injury plays its chief role. Therefore, this model enables us to study the impact of VEGF on repair processes subsequent to initial damage, including reendothelialization and reepithelialization.

In other studies using thalidomide (30) or the VEGFR2 inhibitor SU5416 (29) to ameliorate pulmonary fibrosis, not only angiogenesis but the infiltration of myeloid cells, and therefore the release of various inflammatory and profibrogenic cytokines by these cells, was markedly inhibited. Therefore, these results might be at least partially biased by abrogating the inflammatory phase during the development of pulmonary fibrosis.

We show that ablation of VEGF specifically in myeloid cells leads to aggravated pulmonary fibrosis after pulmonary injury, indicating a protective role of myeloid cell-derived VEGF. The suggested protective role of VEGF secretion by myeloid cells could be attributable to various mechanisms. We show that VEGF inactivation in myeloid cells prevents the formation of blood vessels after pulmonary injury. However, the newly formed vasculature seen in WT control animals likely serves the increased metabolic needs of damaged tissue and enables tissue repair and restoration of homeostasis. Although the repair process is evidently not sufficient to restore tissue homeostasis fully, even in the presence of myeloid cell-derived VEGF, the observation of accelerated fibrosis after inactivation of VEGF in myeloid cells strongly argues that myeloid cell VEGF-driven vascular remodeling is required to retard the development of pulmonary fibrosis. Furthermore, it is possible that myeloid cell-derived VEGF is required as a survival signal for endothelial cells that contributes to the preservation of tissue structure and homeostasis. We observe a striking increase in loss of type II pneumocytes after pulmonary injury in the absence of myeloid cell-derived VEGF. Together with the finding that, overall, pulmonary VEGF levels are drastically reduced in Mut mice, this raises the possibility that VEGF itself serves as a trophic factor for type II pneumocytes that is required for their survival.

A lack of supplying blood vessels can compromise oxygen and nutrient delivery to tissue undergoing repair (31, 32). Hypoxia has

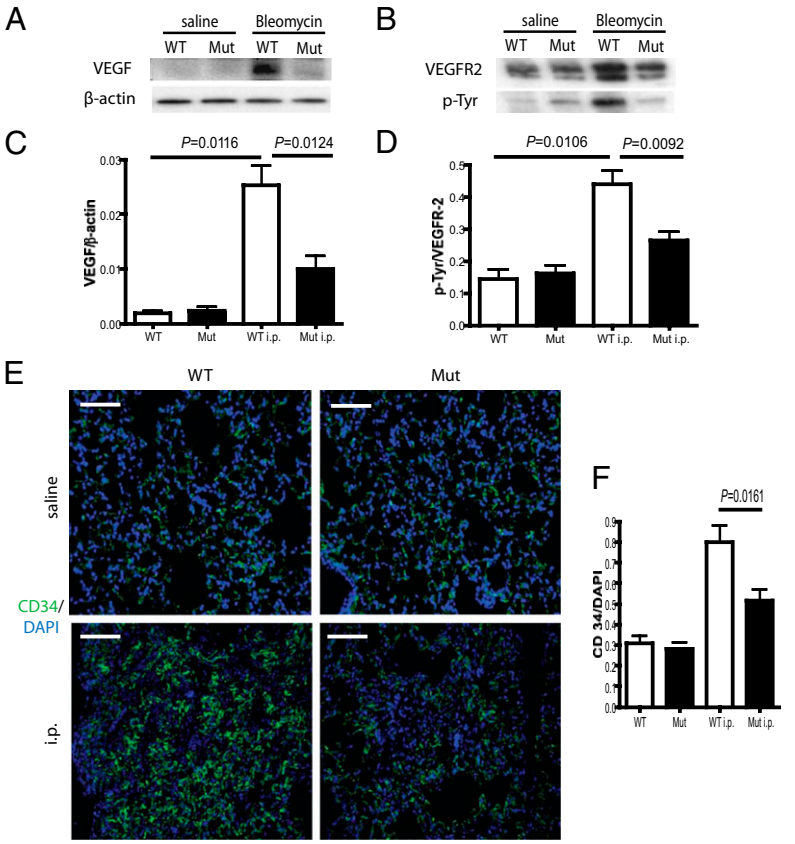

Fig. 3. Ablation of VEGF in myeloid cells results in reduced levels of VEGF, VEGFR2 phosphorylation, and impaired angiogenesis in fibrotic lungs. (*A*) Immunoblotting for VEGF from entire left lung lysates of VEGF Mut and littermate WT mice 21 days after i.p. bleomycin injection or treatment with saline. (*B*) Immunoblotting for VEGFR2 and phosphotyrosine (p-Tyr) after immunoprecipitation of VEGFR2 from entire left lung lysates of Mut and littermate WT mice 21 days after i.p. bleomycin injection or treatment with saline. (*C*) Quantitative analysis of VEGF signals from entire left lung lysates of Mut and WT mice 21 days after i.p. bleomycin injection or treatment with saline as measured by photon emission ($n = 5$). (*D*) Ratio of p-Tyr to VEGFR2 signal from entire left lung lysates of Mut and WT mice 21 days after i.p. bleomycin injection or treatment with saline as a measure of receptor activation ($n = 5$). (*E*) Immunodetection of pulmonary vasculature with the marker CD34 on sections from Mut and WT mice 28 days after i.p. bleomycin injection or treatment with saline. (*F*) Quantitative analysis of the area in pixels covered by CD34 within lung sections from Mut and WT mice 28 days after i.p. bleomycin injection or treatment with saline ($n = 4$). Error bars show SEM. (Scale bars: 100 μm.)

been shown to increase the production of collagen as well as profibrogenic factors like plasminogen activator inhibitor-1, tissue inhibitor of metalloproteinase-1, and connective tissue growth factor through an HIF-mediated transcriptional response (33–35). Furthermore, hypoxia and TGF-β have been shown to synergize with regard to the production of certain collagens in fibroblasts (36, 37). Here, we observed an increase in HIF proteins and in the hypoxia and HIF-regulated marker protein CA-IX after treatment with bleomycin; this increase is much more pronounced in Mut animals. Interestingly, it has been shown that activation of HIF-1 in renal cells is an early event during renal fibrosis and that deletion of HIF-1α prevents fibrotic changes in the kidney (24). Along with the development of pulmonary fibrosis after bleomycin treatment, we observed a down-regulation of E-cadherin, which is, again, more pronounced in VEGF Mut mice. Several studies have reported that HIF-1 as well as HIF-2 is a potent suppressor of E-cadherin expression (38–40). This suggests that a decreased level of tissue perfusion, and accompanying activation of HIFs, is involved in the pathogenesis of pulmonary fibrosis. It further argues that diminished angiogenesis is directly causative of aggravated fibrosis of the lung. Finally, our findings are in agreement with observations from other organs like the kidney and liver, where inhibition of angiogenesis and subsequent hypoxia promoted fibrosis (41, 42).

Fibrotic lungs from animals lacking VEGF in myeloid cells show elevated levels of nuclear β-catenin and cyclin D1, a major downstream component of the Wnt/β-catenin signaling pathway (27), indicating increased Wnt/β-catenin signaling. It has been reported that Wnt/β-catenin signaling can be triggered by hypoxia in an HIF-dependent manner (13, 14) and that the Wnt/β-catenin pathway is involved in the regulation of pulmonary fibroblast proliferation and differentiation of myofibroblasts (5, 16–18). In agreement with these results, we observed increased numbers of myofibroblasts in fibrotic lungs from Mut animals. The increased Wnt/β-catenin signaling observed in VEGF Mut animals is likely a trigger for the increased myofibroblast formation seen in these animals, and this hypothesis is strengthened by observations that fibroblasts transdifferentiate under hypoxic conditions and that resident pulmonary fibroblasts exhibit sustained proliferation after exposure to hypoxia (23).

These data argue that myeloid cells are an indispensable source of VEGF after injury and that vascular remodeling driven by myeloid cell-derived VEGF is required to prevent aberrant fibrotic healing. Although this finding differs from those in studies in which VEGF expression or inhibition is more broadly enacted, it is consistent with the results from a study of a tissue-specific deletion of VEGF in the endothelium that leads to pulmonary fibrosis (43), arguing that tissue-specific delivery of VEGF is an essential aspect of its function in injury. In turn, deletion of VEGF in myeloid cells leads to impaired angiogenesis, with increased activation of HIFs and increased Wnt/β-catenin signaling. Increased signaling through the Wnt/β-catenin pathway triggers the accumulation of myofibroblasts, resulting in aggravated pulmonary fibrosis. Taken together, these observations argue that the process of angiogenesis driven by myeloid cell-derived VEGF is an essential component of tissue repair in the lung, and is therefore a key inhibitor of fibrotic tissue damage.

Materials and Methods

Animals. All animals were housed in an Association for Assessment and Accreditation of Laboratory Animal Care International-approved facility, and animal experiments were conducted in accordance with the National Institutes of Health Guide for the Care and Use of Laboratory Animals.

Targeted deletion of VEGF was created by crossing mice (C57Bl6/J) with both alleles of exon 3 of VEGF-A flanked by loxP sites ($VEGF^{+f/+f}$) (19) into a background of Cre recombinase expression driven by the LysM promoter, which is specific to cells of the myeloid lineage ($LysMCre/VEGF^{+f/+f}$) (20).

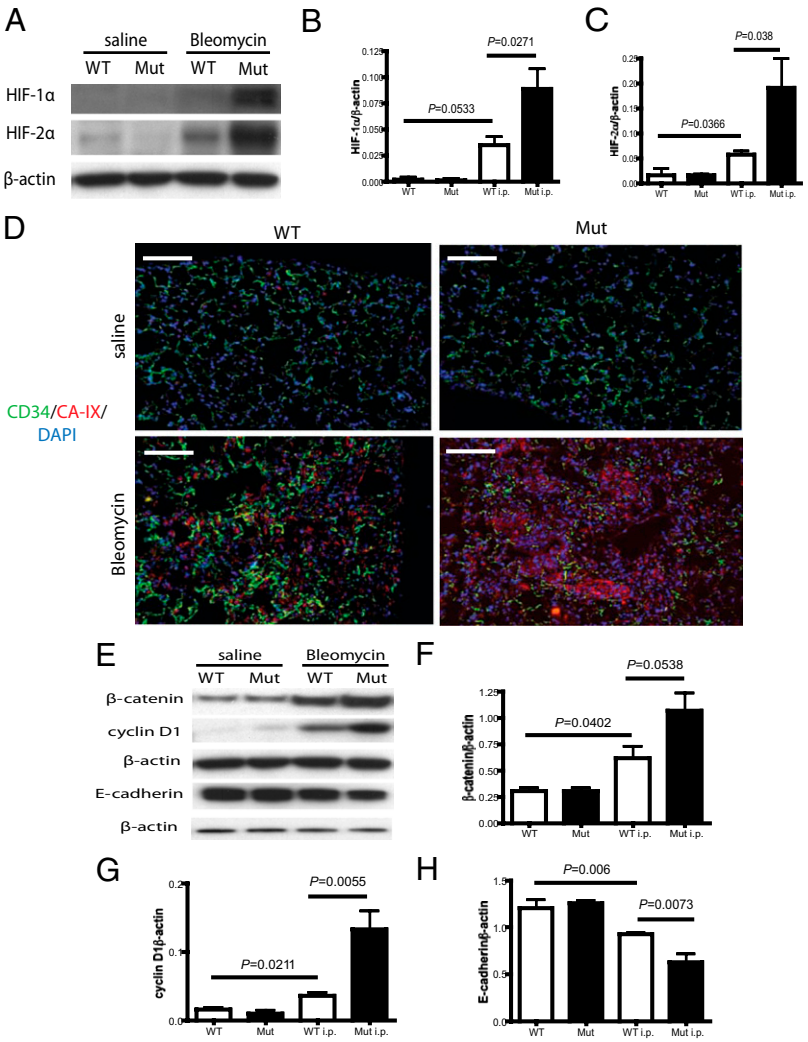

Fig. 4. Increased activation of HIFs and increased Wnt/β-catenin signaling in fibrotic lungs from animals lacking VEGF in myeloid cells. (*A*) Immunoblotting for HIF-1α and HIF-2α from entire left lung nuclear extracts of VEGF Mut or littermate WT mice 21 days after i.p. bleomycin injection or treatment with saline. (*B*) Quantitative analysis of HIF-1α signals from entire left lung nuclear extracts of Mut and WT mice 21 days after i.p. bleomycin injection or treatment with saline as measured by photon emission ($n = 5$). (*C*) Quantitative analysis of HIF-2α signals from entire left lung nuclear extracts of Mut and WT mice 21 days after i.p. bleomycin injection or treatment with saline as measured by photon emission ($n = 5$). (*D*) Simultaneous immunodetection of CD34 and CA-IX in lung sections from Mut and WT mice 28 days after i.p. bleomycin injection or treatment with saline. (*E*) Immunoblotting for β-catenin and cyclin D1 from left lung nuclear extracts and E-cadherin from left lung cytoplasmic extracts of Mut and WT mice 21 days after i.p. bleomycin injection or treatment with saline. (*F*) Quantitative analysis of β-catenin signals from entire left lung nuclear extracts of Mut and WT mice 21 days after i.p. bleomycin injection or treatment with saline as measured by photon emission ($n = 5$). (*G*) Quantitative analysis of cyclin D1 signals from entire left lung nuclear extracts of Mut and WT mice 21 days after i.p. bleomycin injection or treatment with saline as measured by photon emission ($n = 5$). (*H*) Quantitative analysis of E-cadherin signals from entire left lung cytoplasmic extracts of Mut and WT mice 21 days after i.p. bleomycin injection or treatment with saline as measured by photon emission ($n = 5$).

Induction of Pulmonary Injury and Fibrosis. For bleomycin-induced pulmonary fibrosis, female LysMCre Mut mice and WT littermates at 8–12 weeks of age were treated i.p. with bleomycin (10 mg/kg twice weekly; Calbiochem) or saline, and the lungs were collected at the indicated time points.

For histology, the animals underwent cardiac perfusion with PBS/EDTA and 4% (wt/vol) paraformaldehyde (PFA). Before removal, lungs were inflated with 4% PFA and then fixed in 4% (wt/vol) PFA overnight. Alternatively, the left and right lungs were separated and snap-frozen in liquid nitrogen.

Histology, Immunohistochemistry, and Immunofluorescence. For H&E staining, trichrome staining, and immunostaining, 5-μm sections were deparaffinized with xylene and rehydrated with graded ethanol. Antigen retrieval was performed by boiling the sections in citrate buffer for 10 min. The sections were stained according to routine immunohistochemistry procedures and visualized by means of a Vectastain ABC kit (Vector Laboratories).

Primary antibodies used in this study were as follows: biotinylated rat anti-F4/80 at a 1:200 dilution (Serotec), rat anti-CD34 at a 1:200 dilution (Novus), mouse anti-SMA-α at a 1:500 dilution (Chemicon), rabbit anti-TTF-1 at a 1:200 dilution (Abcam), rabbit anti-VEGF at a 1:200 dilution (Calbiochem), rabbit anti-S100A4 (FSP) at a 1:500 dilution (Dako), and rabbit anti-CA-IX at a 1:500 dilution (Novus). The fluorochrome-conjugated Alexa 488 and Alexa 568 (Invitrogen) were used as secondary antibodies.

Quantitative Analysis of Histological Markers. For quantitative analysis of the distribution of immunohistochemical markers within the tissues, sections were photographed into TIFF images using a Leica DMR microscope and SPOT RT color camera system (Diagnostic Instruments, Inc.), and the area (number of pixels) marked by each marker was measured using the Image J program (National Institute of Health) and calculated as the percentage of the area covered by DAPI.

Collagen Assay. The pulmonary collagen content was quantified with a Sircol Assay (Biocolor) according to the manufacturer's instructions.

Oxygen Uptake at the Anaerobic Threshold Measurement. Untrained saline- or bleomycin-treated WT mice and VEGF Mut mice were run on an enclosed-chamber modular treadmill (Columbus Instruments), and the gas flow (O_2

and CO_2) into and out of the chamber treadmill was monitored using the Paramax sensor system (Columbus Instruments) and analyzed using Oxymax software (Columbus Instruments). Mice were run at an initial velocity of 15 m/min, and the velocity was increased by 2 m/min every 2 min. The O_2 uptake and the CO_2 release of the mice were monitored until they reached the anaerobic threshold as indicated by a respiratory exchange rate ≥ 1.

Immunoprecipitation and Immunoblotting. The entire left lung was homogenized in lysis buffer, and Western blotting was performed according to standard procedures. The following antibodies were used: rabbit anti-VEGF (Calbiochem), rabbit anti-HIF-1α (Novus), goat anti-HIF-2α (R&D Systems), mouse anti-β-catenin (BD Biosciences), mouse anti-E-cadherin (BD Biosciences), and mouse anti-β-actin (Sigma). For immunoprecipitation of VEGFR-2, 500 μg of lysate was used. The following antibodies were used in this study: rabbit anti-VEGFR-2 (Santa Cruz) and HRP-conjugated anti-phosphotyrosine (4G10; Millipore). For quantitative analysis, the membranes were scanned with a fluorescence scanner and the signal strength was determined using ImageQuant software (GE Healthcare).

Flow Cytometry. Lungs were removed and cut into small pieces before incubation in a shaker at 37 °C for 45 min in 0.1% Collagenase A (Roche) in RPMI 1640 (Invitrogen). The resulting single-cell suspension was pelleted and rinsed in PBS before treatment with hypotonic lysis buffer and passing through a 70-μm cell strainer (BD Biosciences). One million cells per condition were then incubated with Fc Block (BD Biosciences) before labeling with fluorescently conjugated antibodies using standard protocols. Data were acquired with a FACSCalibur flow cytometer (BD Biosciences) and analyzed with FlowJo software (Tree Star).

Statistical Analysis. Statistical analysis was done using Prism 4.0 software (GraphPad Software). Statistical significance was determined by an unpaired *t* test.

ACKNOWLEDGMENTS. We acknowledge the support of the American Asthma Foundation (V.N and R.S.J.), Deutsche Forschungsgemeinschaft Grant STO 787/1-1 (to C.S.) and Grant WE 2475/1-1 (to A.W.), and National Institutes of Health Grant CA82515 (to R.S.J.).

1. Selman M, King TE, Pardo A; American Thoracic Society; European Respiratory Society; American College of Chest Physicians (2001) Idiopathic pulmonary fibrosis: Prevailing and evolving hypotheses about its pathogenesis and implications for therapy. *Ann Intern Med* 134:136–151.
2. Berse B, Brown LF, Van de Water L, Dvorak HF, Senger DR (1992) Vascular permeability factor (vascular endothelial growth factor) gene is expressed differentially in normal tissues, macrophages, and tumors. *Mol Biol Cell* 3:211–220.
3. Tzouvelekis A, Anevlavis S, Bouros D (2006) Angiogenesis in interstitial lung diseases: A pathogenetic hallmark or a bystander? *Respir Res* 7:82.
4. Simler NR, et al. (2004) Angiogenic cytokines in patients with idiopathic interstitial pneumonia. *Thorax* 59:581–585.
5. Douglas IS, Diaz del Valle F, Winn RA, Voelkel NF (2006) Beta-catenin in the fibroproliferative response to acute lung injury. *Am J Respir Cell Mol Biol* 34:274–285.
6. Farkas L, et al. (2009) VEGF ameliorates pulmonary hypertension through inhibition of endothelial apoptosis in experimental lung fibrosis in rats. *J Clin Invest* 119: 1298–1311.
7. Wang GL, Semenza GL (1995) Purification and characterization of hypoxia-inducible factor 1. *J Biol Chem* 270:1230–1237.
8. Fähling M, Perlewitz A, Doller A, Thiele BJ (2004) Regulation of collagen prolyl 4-hydroxylase and matrix metalloproteinases in fibrosarcoma cells by hypoxia. *Comp Biochem Physiol C Pharmacol Toxicol Endocrinol* 139:119–126.
9. Fähling M, et al. (2006) Translational control of collagen prolyl 4-hydroxylase-alpha(I) gene expression under hypoxia. *J Biol Chem* 281:26089–26101.
10. Bertout JA, Patel SA, Simon MC (2008) The impact of O_2 availability on human cancer. *Nat Rev Cancer* 8:967–975.
11. Tzouvelekis A, et al. (2007) Comparative expression profiling in pulmonary fibrosis suggests a role of hypoxia-inducible factor-1alpha in disease pathogenesis. *Am J Respir Crit Care Med* 176:1108–1119.
12. Bracken CP, et al. (2006) Cell-specific regulation of hypoxia-inducible factor (HIF)-1alpha and HIF-2alpha stabilization and transactivation in a graded oxygen environment. *J Biol Chem* 281:22575–22585.
13. Yang J, Weinberg RA (2008) Epithelial-mesenchymal transition: At the crossroads of development and tumor metastasis. *Dev Cell* 14:818–829.
14. Jiang YG, et al. (2007) Role of Wnt/beta-catenin signaling pathway in epithelial-mesenchymal transition of human prostate cancer induced by hypoxia-inducible factor-1alpha. *Int J Urol* 14:1034–1039.
15. Chilosi M, et al. (2003) Aberrant Wnt/beta-catenin pathway activation in idiopathic pulmonary fibrosis. *Am J Pathol* 162:1495–1502.
16. Kim KK, et al. (2009) Epithelial cell alpha3beta1 integrin links beta-catenin and Smad signaling to promote myofibroblast formation and pulmonary fibrosis. *J Clin Invest* 119:213–224.
17. Königshoff M, et al. (2008) Functional Wnt signaling is increased in idiopathic pulmonary fibrosis. *PLoS One* 3:e2142.
18. Caraci F, et al. (2008) TGF-beta1 targets the GSK-3beta/beta-catenin pathway via ERK activation in the transition of human lung fibroblasts into myofibroblasts. *Pharmacol Res* 57:274–282.
19. Gerber HP, et al. (1999) VEGF is required for growth and survival in neonatal mice. *Development* 126:1149–1159.
20. Clausen BE, Burkhardt C, Reith W, Renkawitz R, Förster I (1999) Conditional gene targeting in macrophages and granulocytes using LysMcre mice. *Transgenic Res* 8: 265–277.
21. Cramer T, Johnson RS (2003) A novel role for the hypoxia inducible transcription factor HIF-1alpha: Critical regulation of inflammatory cell function. *Cell Cycle* 2: 192–193.
22. Stockmann C, et al. (2008) Deletion of vascular endothelial growth factor in myeloid cells accelerates tumorigenesis. *Nature* 456:814–818.
23. Stenmark KR, Gerasimovskaya E, Nemenoff RA, Das M (2002) Hypoxic activation of adventitial fibroblasts: Role in vascular remodeling. *Chest* 122 (6, Suppl):326S–334S.
24. Higgins DF, et al. (2007) Hypoxia promotes fibrogenesis in vivo via HIF-1 stimulation of epithelial-to-mesenchymal transition. *J Clin Invest* 117:3810–3820.
25. Abraham SC, et al. (2002) Solid-pseudopapillary tumors of the pancreas are genetically distinct from pancreatic ductal adenocarcinomas and almost always harbor beta-catenin mutations. *Am J Pathol* 160:1361–1369.
26. Brabletz T, Herrmann K, Jung A, Faller G, Kirchner T (2000) Expression of nuclear beta-catenin and c-myc is correlated with tumor size but not with proliferative activity of colorectal adenomas. *Am J Pathol* 156:865–870.
27. Shtutman M, et al. (1999) The cyclin D1 gene is a target of the beta-catenin/LEF-1 pathway. *Proc Natl Acad Sci USA* 96:5522–5527.
28. Chaudhary NI, et al. (2007) Inhibition of PDGF, VEGF and FGF signalling attenuates fibrosis. *Eur Respir J* 29:976–985.
29. Ou XM, et al. (2009) VEGFR-2 antagonist SU5416 attenuates bleomycin-induced pulmonary fibrosis in mice. *Int Immunopharmacol* 9:70–79.
30. Tabata C, et al. (2007) Thalidomide prevents bleomycin-induced pulmonary fibrosis in mice. *J Immunol* 179:708–714.
31. Horie Y, Wolf R, Russell J, Shanley TP, Granger DN (1997) Role of Kupffer cells in gut ischemia/reperfusion-induced hepatic microvascular dysfunction in mice. *Hepatology* 26:1499–1505.
32. Siegmund SV, Dooley S, Brenner DA (2005) Molecular mechanisms of alcohol-induced hepatic fibrosis. *Dig Dis* 23:264–274.
33. Higgins DF, et al. (2004) Hypoxic induction of Ctgf is directly mediated by Hif-1. *Am J Physiol Renal Physiol* 287:F1223–F1232.
34. Kietzmann T, Roth U, Jungermann K (1999) Induction of the plasminogen activator inhibitor-1 gene expression by mild hypoxia via a hypoxia response element binding the hypoxia-inducible factor-1 in rat hepatocytes. *Blood* 94:4177–4185.
35. Orphanides C, Fine LG, Norman JT (1997) Hypoxia stimulates proximal tubular cell matrix production via a TGF-beta1-independent mechanism. *Kidney Int* 52:637–647.
36. Falanga V, Zhou L, Yufit T (2002) Low oxygen tension stimulates collagen synthesis and COL1A1 transcription through the action of TGF-beta1. *J Cell Physiol* 191:42–50.
37. Saed GM, Zhang W, Chegini N, Holmdahl L, Diamond MP (1999) Alteration of type I and III collagen expression in human peritoneal mesothelial cells in response to hypoxia and transforming growth factor-beta1. *Wound Repair Regen* 7:504–510.
38. Esteban MA, et al. (2006) Regulation of E-cadherin expression by VHL and hypoxia-inducible factor. *Cancer Res* 66:3567–3575.
39. Evans AJ, et al. (2007) VHL promotes E2 box-dependent E-cadherin transcription by HIF-mediated regulation of SIP1 and snail. *Mol Cell Biol* 27:157–169.
40. Krishnamachary B, et al. (2006) Hypoxia-inducible factor-1-dependent repression of E-cadherin in von Hippel-Lindau tumor suppressor-null renal cell carcinoma mediated by TCF3, ZFHX1A, and ZFHX1B. *Cancer Res* 66:2725–2731.
41. Kang DH, Johnson RJ (2003) Vascular endothelial growth factor: A new player in the pathogenesis of renal fibrosis. *Curr Opin Nephrol Hypertens* 12:43–49.
42. Patsenker E, et al. (2009) Pharmacological inhibition of integrin alphavbeta3 aggravates experimental liver fibrosis and suppresses hepatic angiogenesis.. *Hepatology* 50:1501–1511.
43. Lee S, et al. (2007) Autocrine VEGF signaling is required for vascular homeostasis. *Cell* 130:691–703.